THE JOURNAL OF BIOLOGICAL CHEMISTRY VOL. 283, NO. 43, pp. 29069–29076, October 24, 2008

Functional Role of HSP90 Complexes with Endothelial Nitric-oxide Synthase (eNOS) and Calpain on Nitric Oxide Generation in Endothelial Cells*

Received for publication, May 12, 2008, and in revised form, July 23, 2008 Published, JBC Papers in Press, August 5, 2008, DOI 10.1074/jbc.M803638200

Monica Averna, Roberto Stifanese, Roberta De Tullio, Mario Passalacqua, Franca Salamino, Sandro Pontremoli, and Edon Melloni[1]

From the Department of Experimental Medicine (DIMES), Biochemistry Section, and Centre of Excellence for Biomedical Research (CEBR), University of Genoa, Viale Benedetto XV, 1-16132 Genoa, Italy

Although several reports have indicated that eNOS is a highly sensitive calpain substrate, the occurrence of a concomitant Ca^{2+}-dependent activation of the synthase and of the protease has never been analyzed in specific direct experiments. In this study, we have explored *in vivo* how eNOS can undergo Ca^{2+}-dependent translocation and activation, protected against degradation by activated calpain. Here we demonstrate that following a brief exposure to Ca^{2+}-loading, the cytosolic eNOS-HSP90 complex recruits calpain in a form in which the chaperone and the synthase are almost completely resistant to digestion by the protease. Furthermore, in the presence of the HSP90 inhibitor geldanamycin, a significant decrease in NO production and an extensive degradation of eNOS protein occurs, indicating that dissociation from membranes and association with the chaperone is correlated to the protection of the synthase. Experiments with isolated membrane preparations confirm the primary role of HSP90 in dissociation of eNOS from caveolae. Prolonged exposure of cells to Ca^{2+}-loading resulted in an extensive degradation of both eNOS and HSP90, accompanied by a large suppression of NO production. We propose that the protective effect exerted by HSP90 on eNOS degradation mediated by calpain represents a novel and critical mechanism that assures the reversibility of the intracellular trafficking and activation of the synthase.

The endothelial form of nitric-oxide synthase (eNOS)[2] is known to be present in resting cells associated with caveolae, interacting in an inactive form with caveolin-1 (1–6). Thus, dissociation from caveolae is the initial obligatory step of the overall activation process of eNOS required to remove the synthase from caveolin-1 inhibition. This mechanism is triggered by a $[Ca^{2+}]_i$ elevation and requires interaction of eNOS with both calmodulin (CAM) and HSP90 (7–15). These sequential reactions have been proposed on the basis of observations obtained mainly with immunoprecipitation experiments and using recombinant proteins (11, 14, 15). Furthermore, it is well known that eNOS is a sensitive calpain substrate (16–21) and that the elevation of $[Ca^{2+}]_i$ required for the initiation of the eNOS activation cycle also induces the activation of this protease through its translocation to the membranes (22–25). It must be emphasized that several reports have described the proteolytic degradation of NO synthases, but its occurrence has been related to an intense intracellular Ca^{2+} overload induced by exocytotic conditions or the removal of incorrectly folded NO synthase molecules. In this respect, it has been reported that HSP90 can affect the proteolysis of eNOS by regulating heme insertion and formation of the active dimeric enzyme form.

At present, very little is known about the regulation of eNOS trafficking between different subcellular compartments. However, on the basis of the above considerations, it can be assumed that an efficient *in vivo* mechanism must be operating to protect the synthase in its native active state from uncontrolled calpain-mediated proteolysis, which could markedly reduce eNOS activity.

In previous studies (16, 17), we have demonstrated that in the presence of Ca^{2+}, calpain can be recruited in a ternary complex containing eNOS, HSP90, and the protease. In this associated form, HSP90 and NOS become resistant to calpain digestion. We have also shown that in intact cells and in rat tissues, the level of HSP90 expression is directly correlated with the extent of NOS degradation. Accordingly, in rat aorta, under conditions of calpain activation, endothelial NOS is much more vulnerable to proteolytic degradation than neuronal NOS (17), since HSP90 is more abundant in brain.

In the present study, we have further explored in Ca^{2+}-loaded endothelial cells the role of HSP90 in: (i) the protection of eNOS from calpain digestion, (ii) the intracellular redistribution of the synthase, and (iii) the control of NO production.

We are now reporting that following an increase in $[Ca^{2+}]_i$ induced by Ca^{2+}-ionophore or acetylcholine treatment, eNOS dissociates from caveolin-1 and translocates to the cytosol. Under these conditions, no changes in the intracellular distribution of HSP90 occurred because the bulk of the chaperone remained largely diffused in the cytosol. Disruption of the

*This work was supported in part by grants from MIUR, FIRB, and PRIN projects, and from the University of Genoa. The costs of publication of this article were defrayed in part by the payment of page charges. This article must therefore be hereby marked "*advertisement*" in accordance with 18 U.S.C. Section 1734 solely to indicate this fact.

[1] To whom correspondence should be addressed: DIMES-Biochemistry Section, Viale Benedetto XV, 1-16132 Genoa. Tel.: 39-010-3538128; Fax: 39-010-518343; E-mail: melloni@unige.it.

[2] The abbreviations used are: eNOS, endothelial nitric-oxide synthase; mAb, monoclonal antibody; CAM, calmodulin; L-NAME, *N*-nitro-L-arginine methyl ester.

eNOS-caveolin-1 interaction was accompanied by its activation and by NO production. In isolated membrane preparations, the release of eNOS required the presence of HSP90; Ca^{2+}-CAM alone is significantly less efficient. In the presence of the HSP90 inhibitor geldanamycin, NO production was largely decreased, and the synthase was extensively degraded. Immunoprecipitation of HSP90 from cell lysates revealed that only in Ca^{2+}-loaded cells, cytosolic diffusion of eNOS was accompanied by the formation of an eNOS-HSP90-calpain heterotrimeric complex.

Taken together, these results indicate a novel role of HSP90 that operates *in vivo* in protecting eNOS from calpain-mediated degradation in the course of the intracellular dynamic redistribution that accompanies the enzyme activation and NO production.

We are herewith proposing that HSP90 participates in the eNOS activation cycle, not only through its role in dissociation and stabilization of the active synthase form, but also for its crucial effect in preserving the enzyme from proteolytic degradation by calpain.

EXPERIMENTAL PROCEDURES

Materials—Leupeptin, aprotinin, phosphatase inhibitor mixture I and II, calmodulin, 4,5-diamino-fluorescein diacetate (DAF-2DA), Ca^{2+}-ionophore A23187, *N*-nitro-L-arginine methyl ester (L-NAME), calpain inhibitor-1, ATP, phosphoenolpyruvate, pyruvate kinase, and acetylcholine chloride were purchased from Sigma Aldrich. 4-(2-aminoethyl) benzenesulfonylfluoride (AEBSF) and geldanamycin were obtained from Calbiochem. ECL® Detection System was obtained from GE Healthcare. *t*-Boc-Leu-Met-CMAC fluorogenic calpain substrate (26) was purchased from Molecular Probes (Invitrogen).

Antibodies—Monoclonal mouse IgG1 eNOS and HSP90 antibodies and polyclonal rabbit caveolin antibody were purchased from BD Transduction Laboratories, Milan, Italy; serum μ-calpain (mAb 56.3) antibody was produced as described in Ref. 27.

Cell Culture—bEnd5 cells were kindly provided by L. Riboni (Department of Medical Chemistry, Biochemistry and Biotechnology, University of Milan, LITA-Segrate, Milan, Italy) and maintained in continuous culture at 37 °C (5% CO_2) with Dulbecco's modified Eagle's medium growth medium containing 10% fetal bovine serum, 10 units·ml^{-1} penicillin, 100 μg·ml^{-1} streptomycin, 2 mM L-glutamine, 1 mM sodium pyruvate, all purchased from Sigma Adrich.

Immunofluorescence Confocal Microscopy and Fluorescence Quantification—bEnd5 cells grown on glass slides (8×10^4 cells) were fixed and permeabilized by the Triton/paraformaldehyde method, as described in Ref. 28. Cells were treated with 2.5 μg/ml eNOS, or HSP90 or caveolin antibodies diluted in phosphate-buffered saline solution containing 5% (v/v) fetal-calf serum. After incubation for 3 h at room temperature, cells were washed three times with phosphate-buffered saline and treated with 4 μg/ml chicken anti-mouse Alexa fluor 488 conjugate or 4 μg/ml chicken anti-rabbit Alexa fluor 568 conjugate (Molecular Probes) secondary antibodies for 1 h. Images were collected by a Bio-Rad MRC1024 confocal microscopy, using a 60× Plan Apo objective with numerical aperture 1.4. Sequential acquisitions were performed to avoid cross-talk between color channels. The fluorescence intensity in each collected image was quantified using LaserPix software (Bio-Rad) and followed the procedure described in Ref. 29.

Immunoprecipitation and Immunoblot—bEnd5 cells (1×10^6 cells) treated as described elsewhere in this report were lysed by three cycles of freezing and thawing in 500 μl of ice-cold 20 mM Tris/HCl, 2.5 mM EDTA, 2.5 mM EGTA, 0.14 M NaCl, 10 μg/ml aprotinin, 20 μg/ml leupeptin, AEBSF 10 μg/ml, phosphatase inhibitor mixture I and II 10 μg/ml, pH 7.4 (immunoprecipitation buffer). Cell lysates were centrifuged at $12{,}000 \times g$ for 15 min at 4 °C, and protein quantification of the supernatants was performed using the Lowry method (30). To perform the immunoprecipitations, 500 μg of soluble protein (crude extract) has been precleared with protein G-Sepharose, and then incubated in the presence of 2 μg of anti-HSP90 mAb at 4 °C, overnight. Protein G-Sepharose was then added to each sample and incubated for an additional 1 h. The immunocomplexes were washed three times with immunoprecipitation buffer without enzyme inhibitors, heated in SDS-PAGE loading buffer for 5 min, and run on 6% SDS-PAGE (31). Proteins were then transferred by electroblotting onto a nitrocellulose membrane and saturated with phosphate-buffered saline, pH 7.5, containing 5% skim milk powder. The blots were probed with specific antibodies, followed by a peroxidase-conjugated secondary antibody as previously described and then developed with an ECL detection system (32). The immunoreactive material was detected with a Bio-Rad Chemi Doc XRS apparatus and quantified using the Quantity One 4.6.1 software (Bio-Rad). The procedure was quantitated using known amounts of proteins submitted to SDS-PAGE and detected with the appropriate antibody. The bands obtained were scanned and used to create a calibration curve.

Determination of NO Production with DAF-2DA—bEnd5 cells (2×10^4 cells) grown on a 96-well microplate were incubated at 37 °C for 30 min in 200 μl of ice-cold oxygenated physiological salt solution having the following composition: 10 mM HEPES, 0.14 M NaCl, 5 mM KCl, 5 mM glucose, 1 mM $MgCl_2$, pH 7.4 (HEPES buffer) containing 100 μM L-arginine and 5 μM DAF-2DA. This compound is non-fluorescent but reacts with NO in the presence of oxygen to form the highly fluorescent derivative DAF-2 triazole (33, 34), whose intensity is proportional to NO levels. The cells were then rinsed twice with HEPES buffer and after the addition of 1 μM calcium ionophore A23187 in 200 μl of HEPES buffer containing 2 mM $CaCl_2$ in the absence or presence of 1 mM L-NAME, the fluorescence (excitation wavelength 485 nm; emission wavelength 535 nm) was continuously measured using the top reading mode in the fluorescence multilabel reader LB 940 Mithras, Berthold, Germany.

Assay of Intracellular Calpain Activity—bEnd5 cells (2×10^4 cells) grown on a 96-well microplate were incubated at 37 °C for 20 min in 200 μl of ice-cold oxygenated HEPES buffer containing 50 mM *t*-Boc-Leu-Met-CMAC fluorogenic calpain substrate and 2 mM $CaCl_2$. Cells were then washed twice with HEPES buffer to remove excess substrate, and after the addition of 1 μM calcium ionophore A23187 in 200 μl of HEPES buffer

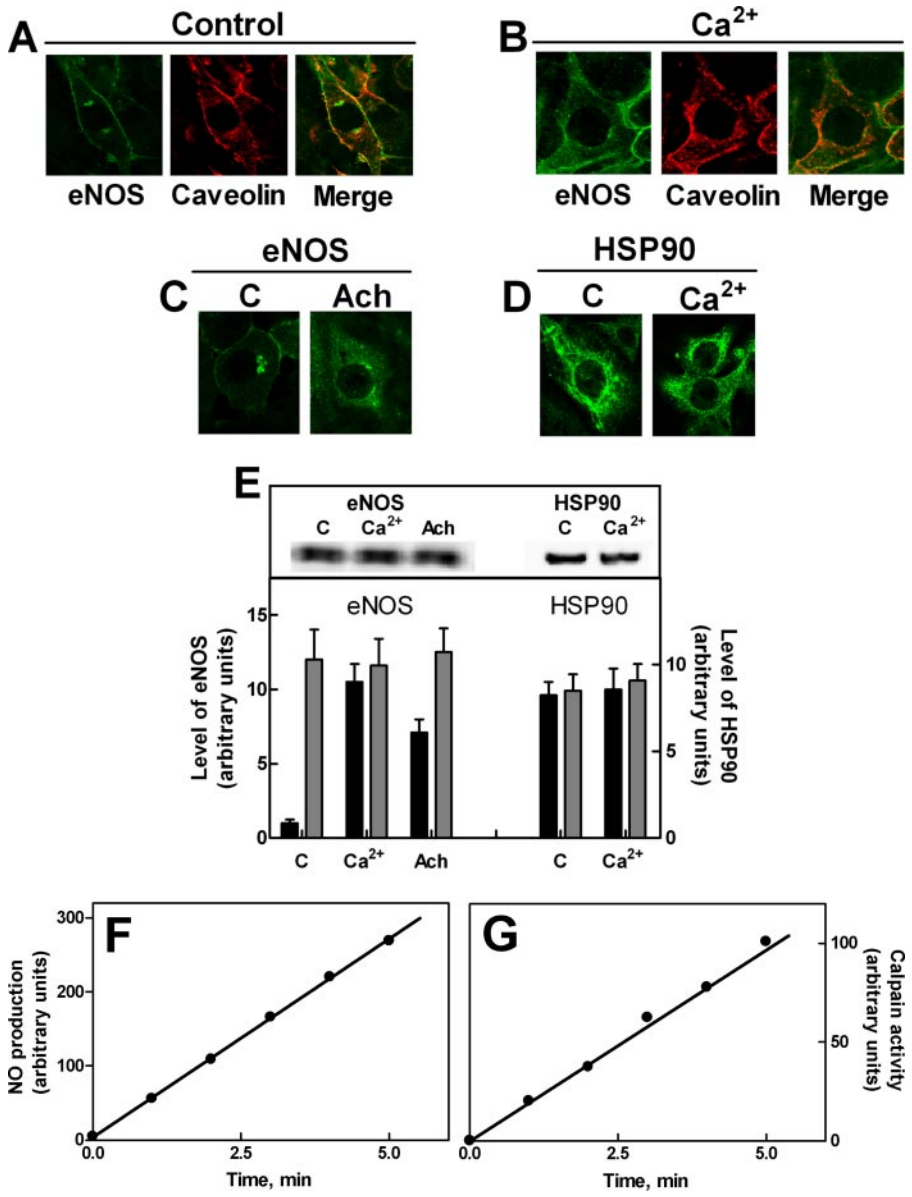

FIGURE 1. **Effect of an increase in intracellular free calcium on eNOS and HSP90 localization in bEnd5 cells.** *A* and *B*, bEnd5 cells grown on glass slides (8×10^4 cells) as described under "Experimental Procedures" were treated in the absence (*A*) or presence (*B*) of 1 μM Ca^{2+}-ionophore A23187 for 5 min. In *C*, the cells were treated in the absence (*C*) or presence of 1 μM acetylcholine (*Ach*) for 30 min. In *D*, the cells were treated in the absence (*C*) or presence of 1 μM Ca^{2+}-ionophore A23187 for 5 min (Ca^{2+}). After treatment, eNOS, caveolin, and HSP90 localizations were determined by confocal microscopy using the specific antibodies as described under "Experimental Procedures." In the third image of *panels A* and *B* (merge), the *yellow* staining indicates co-localization of the two proteins detected. The images are representative of six different experiments. *E*, bEnd5 cells (1×10^5) were left untreated (*C*) or treated in the presence of 1 μM Ca^{2+}-ionophore A23187 for 5 min (Ca^{2+}) or 1 μM acetylcholine (*Ach*) for 30 min were lysed in 100 μl of SDS-PAGE loading buffer, heated for 5 min at 95 °C, and aliquots of each sample (30 μl) were submitted to SDS-PAGE (6%) and Western blot analysis. HSP90 and eNOS were detected using the specific antibodies. The immunoreactive bands were quantified as described under "Experimental Procedures" (*gray bars*). The cytosolic fluorescence of eNOS and HSP90 derived from the images reported in *A*, *B*, *C*, and *D* was quantified as described under "Experimental Procedures" (*black bars*). The values of each quantification are the arithmetical mean ± S.D. of three different experiments. *F*, bEnd5 cells (2×10^4 cells) were loaded for 30 min at 37 °C with DAF-2 DA and incubated with 1 μM Ca^{2+}-ionophore A23187. eNOS activity was assessed as the L-NAME-dependent increase in fluorescence (see "Experimental Procedures") at the indicated times of incubation. The values are the arithmetical mean of three determinations. *G*, bEnd5 cells (2×10^4 cells) were loaded for 20 min at 37 °C with the cell-permeable fluorogenic *t*-Boc-Leu-Met-CMAC calpain substrate and incubated with 1 μM Ca^{2+}-ionophore A23187. Fluorescence was recorded as described under "Experimental Procedures." The values are the arithmetical mean of three determinations.

containing 2 mM $CaCl_2$, the fluorescence emission was continuously monitored with a Mithras LB 940 plate reader (Berthold Technologies). The excitation/emission wavelengths were 355/485 nm, respectively.

Detection of eNOS from Isolated Endothelial Cell Membranes—bEnd5 cells (1×10^6 cells) were collected and lysed with three cycles of freezing and thawing in 500 μl of ice-cold immunoprecipitation buffer. Cell lysates were centrifuged at 100,000 × *g* for 15 min at 4 °C, and the particulate material was washed 3-fold with HEPES buffer, adding 0.01% Triton X-100 in the last washing. After centrifugation at 100,000 × *g* for 5 min, membranes were incubated (100 μl) under different conditions for 30 min at 4 °C and centrifuged again at 100,000 × *g* for 15 min. The supernatants and the membranes of each sample were heated in SDS-PAGE loading buffer for 5 min, and aliquots (30 μl) were submitted to 6% SDS-PAGE (31). Proteins were then transferred by electroblotting onto a nitrocellulose membrane, and eNOS was detected as described above.

RESULTS

Subcellular Translocation of eNOS in Ca^{2+}-loaded Cells—Previous reports (14, 35, 36) have indicated that dissociation of eNOS from caveolae is an essential step in the synthase activation process. To better define the biochemical relevance of this process, we have analyzed by confocal microscopy the changes in eNOS localization under conditions of an increased $[Ca^{2+}]_i$, also promoting activation of the enzyme. In resting cells, co-immunolocalization experiments revealed that eNOS is mostly associated with caveolin-1 protein, present in both plasma membranes and the Golgi apparatus (Fig. 1*A*). Following an increase in $[Ca^{2+}]_i$ induced by cell treatment with the Ca^{2+} ionophore, eNOS dissociates from membranes and becomes detectable as a diffused cytosolic enzyme, no longer co-localized with caveolin-1 (Fig. 1*B*). Identical results were also obtained by stimulation with the natural agonist acetylcholine, which promotes an increase in free $[Ca^{2+}]_i$ through its mobilization from intracellular stores (Fig. 1*C*).

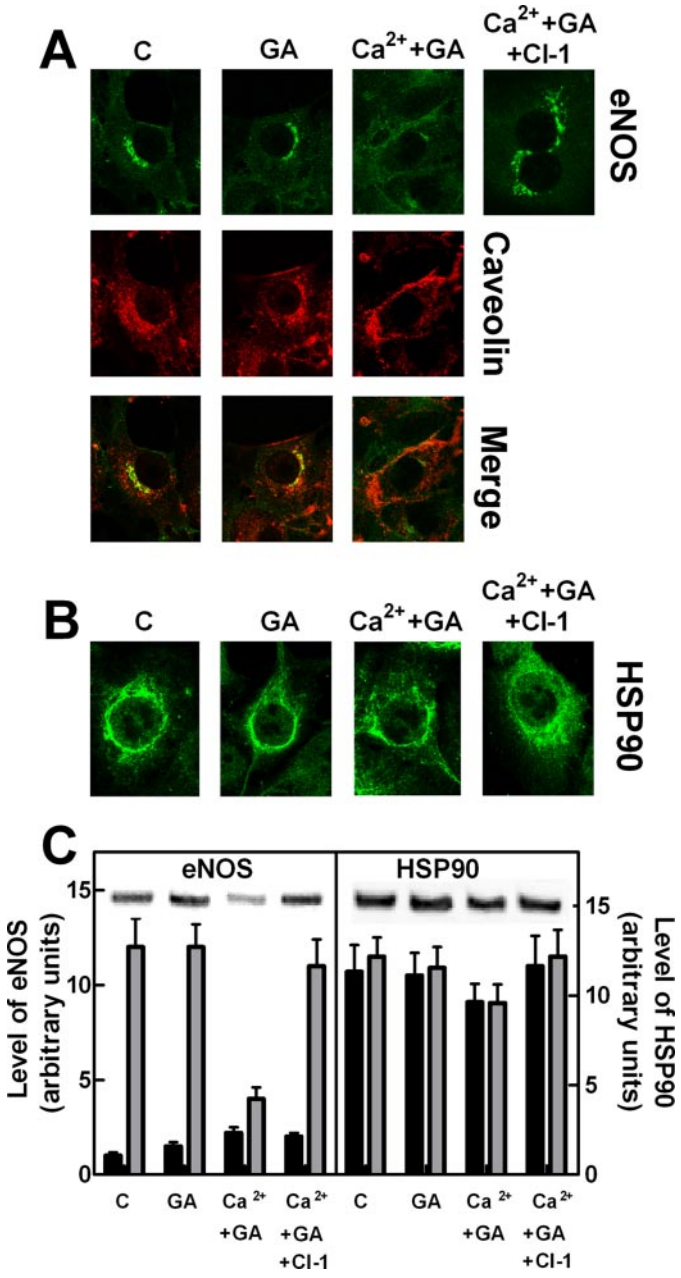

FIGURE 2. **Effect of geldanamycin on eNOS and HSP90 localization in bEnd5 cells.** bEnd5 cells grown on glass slides (8×10^4 cells) as described under "Experimental Procedures" were left untreated (*C*), or were treated with 100 nM geldanamycin alone (*GA*) or followed by an incubation with 1 μM Ca^{2+}-ionophore A23187 for 5 min (Ca^{2+}+GA). Alternatively, the cells treated with 100 nM geldanamycin were also incubated with 1 μM calpain inhibitor-1 for 30 min, followed by an incubation with 1 μM Ca^{2+}-ionophore A23187 for 5 min (*Ca^{2+}+GA+Cl-1*). After treatment, eNOS and caveolin (*A*) and HSP90 (*B*) localizations were determined by confocal microscopy using the specific antibodies as described under "Experimental Procedures." The images are representative of six different experiments. *C*, bEnd5 cells (1×10^5) were submitted to the same experimental procedures carried out in *A*. After treatment, cells were lysed in SDS-PAGE loading solution (100 μl) under the same conditions reported in the legend to Fig. 1*E*. Aliquots (30 μl) of each sample were used for Western blot analysis. HSP90 and eNOS were detected using the specific antibodies. The immunoreactive bands detected in *C* were quantified as described under "Experimental Procedures" (*gray bars*). The cytosolic fluorescence of eNOS and HSP90 derived from the images reported in *A* and *B* were quantified as described under "Experimental Procedures" (*black bars*). The values of each quantification are the arithmetical mean ± S.D. of three different experiments.

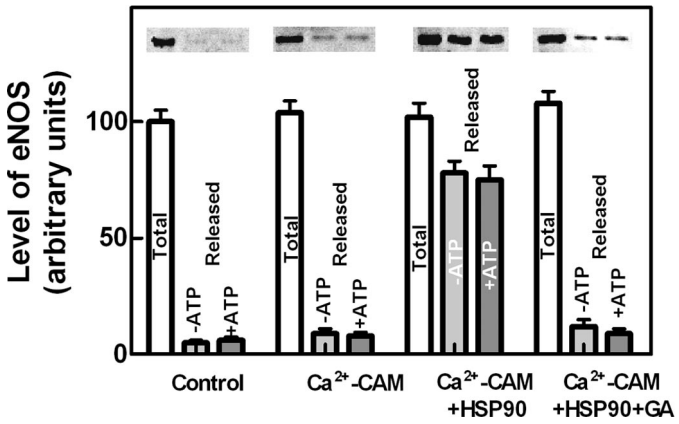

FIGURE 3. **Mobilization of eNOS from isolated endothelial cell membranes.** Isolated bEnd5 endothelial cell membranes prepared as described under "Experimental Procedures" were incubated for 30 min at 4 °C in HEPES buffer alone (*Control*) or containing 0.1 mM $CaCl_2$ + 1 μM CAM (Ca^{2+}-CAM) or containing 0.1 mM $CaCl_2$ + 1 μM CAM + 15 μg of purified HSP90 (17) in the absence (Ca^{2+}-CAM + HSP90) or in the presence (Ca^{2+}-CAM + HSP90 + GA) of 100 nM geldanamycin, and centrifuged at 100,000 × *g* for 15 min. The supernatants (*Released*) and the membranes (*Total*) of each sample were submitted to SDS-PAGE and Western blot analysis and eNOS was detected using the specific antibody. These experiments were performed in the absence (−*ATP*) or in the presence (+*ATP*) of 2 mM Mg-ATP, together with 10 mM phosphoenolpyruvate and 2 μg of purified pyruvate kinase, to maintain the level of ATP. The immunoreactive bands were quantified as described under "Experimental Procedures." The values of each quantification are the arithmetical mean ± S.D. of three different experiments.

In both resting and Ca^{2+}-stimulated cells, the bulk of HSP90 remains preferentially distributed in the soluble cytosolic fraction without changes in its protein level (Fig. 1, *D* and *E*). Dissociation from the membranes and diffusion of eNOS into the cytosol is not accompanied by changes in the total level of eNOS protein (Fig. 1*E*) and therefore the large increase in the fluorescence can be attributed to the large fraction of eNOS molecules translocated from caveolae to cytosol.

During a brief period of Ca^{2+}-loading, eNOS activity becomes detectable, confirming that the enzyme redistribution is part of its activation mechanism (Fig. 1*F*). Under these conditions, the hydrolysis of a cell-permeable calpain substrate (Fig. 1*G*) also occurred, indicating that the protease has undergone activation. However, it is interesting to note that, under these conditions, no degradation of eNOS and HSP90 could be detected, indicating that both proteins were protected from Ca^{2+}-dependent proteolysis.

eNOS Protection in Ca^{2+}-loaded Cells—To correlate the changes in intracellular eNOS localization with its activation and protection from calpain digestion, the steps of the eNOS activation mechanism involved in such a protective process were investigated. Following the addition of the HSP90 inhibitor geldanamycin (37–44) to Ca^{2+}-loaded cells, the fluorescence of eNOS associated to the membranes is largely decreased, and only a small amount of eNOS becomes detectable in the cytosolic fraction (Fig. 2*A*). Immunoblotting analysis revealed that more than 60–70% of the total amount of eNOS protein had been degraded (Fig. 2*C*). Under these conditions, HSP90 was only 10–15% digested with respect to the initial amount (Fig. 2*C*). These degradation processes occurring in Ca^{2+}-loaded cells in the presence of geldanamycin were mediated by active calpain, as indicated by the recovery of both

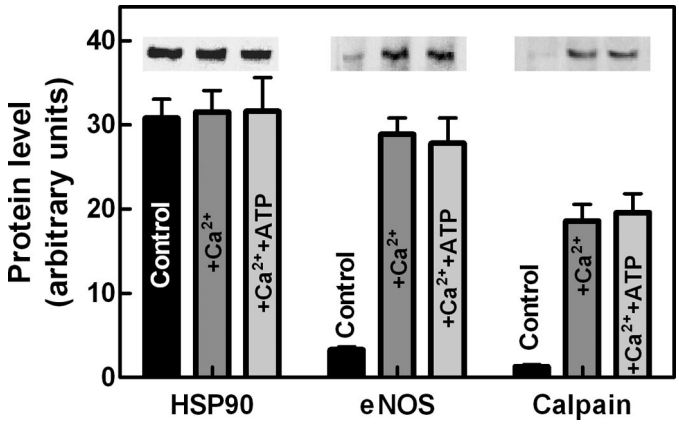

FIGURE 4. **Effect of an increase in intracellular free calcium on the association of eNOS and calpain with HSP90.** bEnd5 cells (1×10^6 cells) left untreated (*Control*) or treated with 1 μM Ca^{2+}-ionophore A23187 for 5 min at 37 °C in the absence ($+Ca^{2+}$) or in the presence of 2 mM Mg-ATP, together with 10 mM phosphoenolpyruvate and 2 μg of purified pyruvate kinase ($+Ca^{2+}+ATP$) were lysed, and aliquots (500 μg of soluble protein) obtained as described under "Experimental Procedures" were incubated overnight at 4 °C with monoclonal anti-HSP90 antibody. The mixtures were then incubated for 1 h at 4 °C with protein G-Sepharose (30 μl). The particles were collected, washed three times with the immunoprecipitation buffer, resuspended in SDS/PAGE loading solution (30 μl), and submitted to 6% SDS/PAGE. The presence in the solubilized material of eNOS and calpain together with HSP90 was established using the specific mAbs. The immunoreactive bands of each protein were quantified as described under "Experimental Procedures." The values of each quantification are the arithmetical mean ± S.D. of three different experiments.

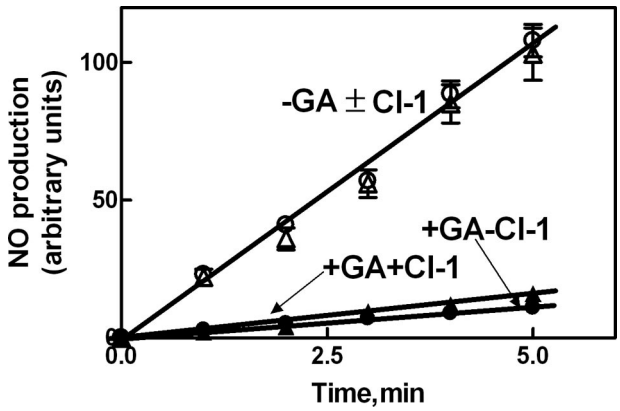

FIGURE 5. **Effect of geldanamycin and calpain inhibitor-1 on eNOS activity in bEnd5 cells.** bEnd5 cells (2×10^4 cells) were loaded for 30 min at 37 °C with DAF-2 DA as described under "Experimental Procedures" and incubated with 1 μM Ca^{2+}-ionophore A23187 in the absence (*filled circles*) or presence (*unfilled circles*) of 100 nM geldanamycin. These experiments were also performed with the addition of 1 μM calpain inhibitor-1 (*+CI-1*). GA and CI-1 were added 30 min before the specific stimulus. eNOS activity was assessed as the L-NAME-dependent increase in fluorescence (see "Experimental Procedures") at the indicated times of incubation.

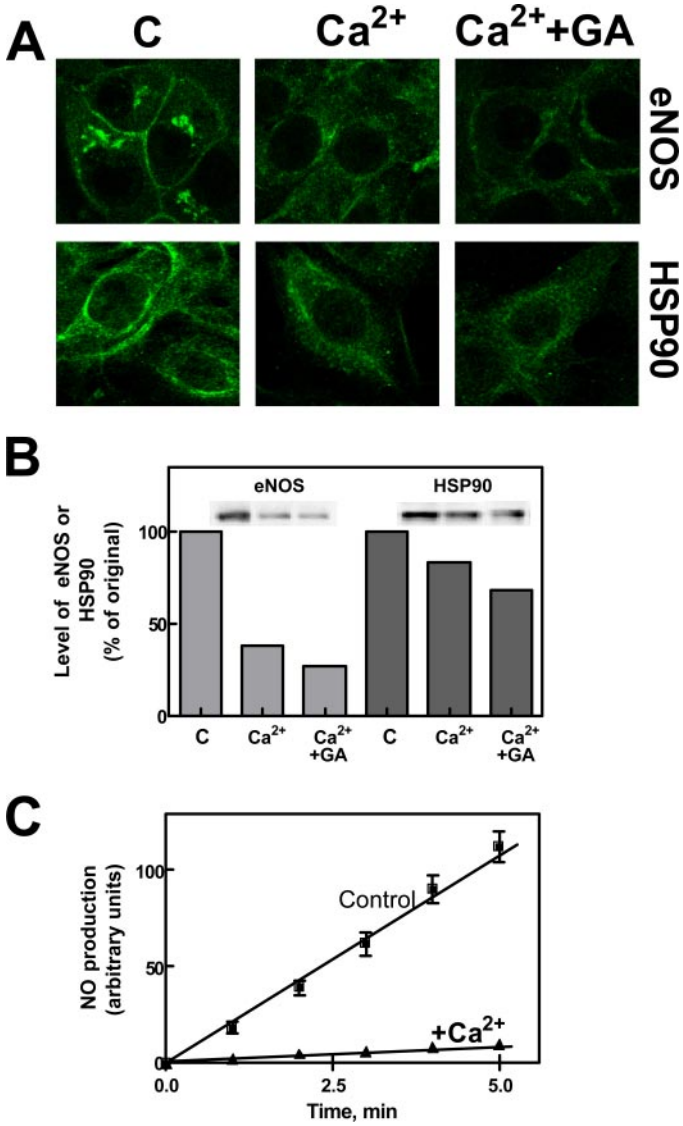

FIGURE 6. **Effect of a prolonged increase in intracellular free calcium on eNOS and HSP90 protein levels.** *A*, bEnd5 cells grown on glass slides (8×10^4 cells) were left untreated (*C*), or were treated with 1 μM Ca^{2+}-ionophore A23187 for 30 min in the absence (Ca^{2+}) or in the presence of 100 nM geldanamycin (Ca^{2+} + *GA*). Geldanamycin was added 30 min before the specific stimulus. After treatment, eNOS and HSP90 localization was determined by confocal microscopy using the specific antibodies as described under "Experimental Procedures." *B*, bEnd5 cells (1×10^5) submitted to the same experiments carried out in *A*, were lysed in SDS-PAGE loading solution (100 μl) under the same conditions reported in the legend to Fig. 1*E*. Aliquots of each sample (30 μl) were used for Western blot analysis, and the immunoreactive bands were quantified as described under "Experimental Procedures." *C*, bEnd5 cells (2×10^4) were loaded for 30 min at 37 °C with DAF-2 DA as described under "Experimental Procedures" and then incubated in the absence (*Control*) or presence of 1 μM Ca^{2+}-ionophore A23187 ($+Ca^{2+}$) for 30 min. After treatment, eNOS activity was assessed as the L-NAME-dependent increase in fluorescence at the indicated times of incubation.

eNOS and HSP90 proteins in cells treated with the synthetic calpain inhibitor CI-1 (Fig. 2). Thus, following inhibition of HSP90, both diffusion into the cytosol and protection of eNOS from calpain degradation are prevented. To better characterize the role of HSP90 in these processes, we have evaluated the role of the chaperone protein in dissociation of eNOS from isolated membranes as well as in the formation of soluble protein complexes. As shown in Fig. 3, a very low amount of eNOS was displaced from membranes following the addition of Ca^{2+}-CAM, whereas in the concomitant presence of isolated HSP90, a large release of eNOS was observed. The presence of ATP did not modify the extent of release, but that of geldanamycin reduced almost completely the release of eNOS from membranes, suggesting that the ATPase activity of HSP90 (42, 45–47) is not required for this effect of the chaperone molecule.

These observations could be explained on the basis of the well defined property of HSP90 to bind eNOS, forming discrete complexes (11, 17, 19). Similarly, we have previously observed

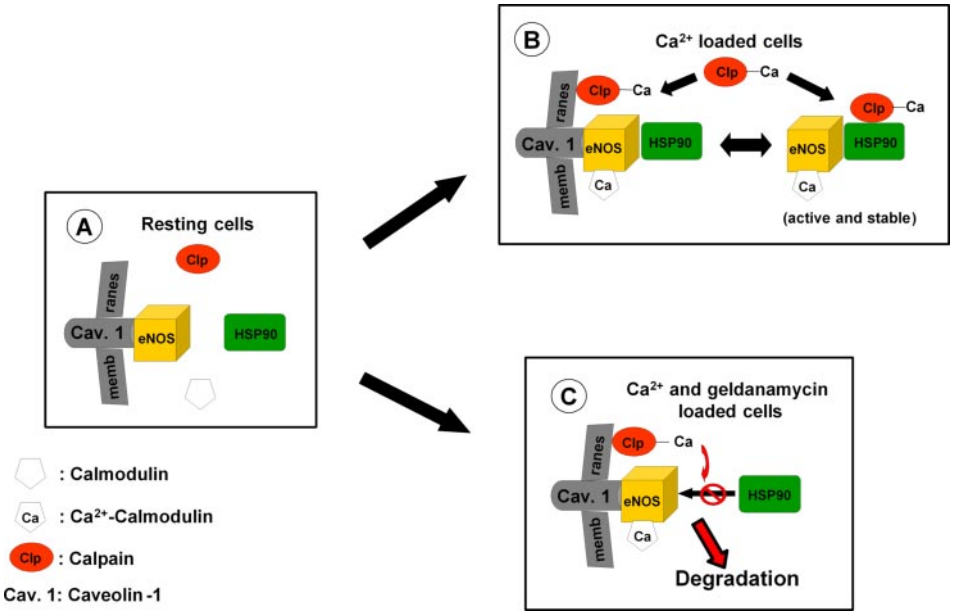

FIGURE 7. **Proposed model for the role of HSP90 in the eNOS activation cycle.** *A*, in resting cells, eNOS is associated in an inactive form to caveolin-1. *B*, following a rise in intracellular [Ca^{2+}], interaction of eNOS with Ca^{2+}-CAM and with HSP90 promotes the dissociation of the synthase from caveolin-1 and its activation in the cytosol. The reversibility of this process is assured by the formation of a HSP90-eNOS-calpain heterocomplex resistant to proteolysis. *C*, in the absence of active HSP90, the complex formation does not occur, and eNOS becomes highly susceptible to degradation by active calpain.

that in the presence of Ca^{2+}, the eNOS-HSP90 complex can recruit calpain generating a ternary complex in which both eNOS and HSP90 were resistant to degradation by the endogenous calpain (17). Thus, the formation of such a ternary complex was analyzed by means of the immunoprecipitation of cytosolic HSP90. As shown in Fig. 4, in the soluble fraction of resting cells, despite the high availability of HSP90, no co-immunoprecipitation of eNOS was detected, in accordance with the observations shown in Fig. 1, indicating that almost all eNOS is present in a particulate form. Following cell-loading with Ca^{2+}, immunoprecipitation experiments revealed the presence in the soluble fraction of complexes containing in addition to HSP90, eNOS and calpain. The formation of these complexes was not affected by the presence of ATP.

Thus, HSP90 plays a dual role: (i) promoting the release of the Ca^{2+}-CAM-eNOS complex from caveolin-1, a step liberating the synthase from its natural inhibitor, and (ii) protecting eNOS from calpain digestion in the cytosol. The removal of eNOS from membranes and the recruitment of calpain into the eNOS-HSP90 complexes are both involved in the maintenance of an active synthase form.

This is supported by the results shown in Fig. 5 indicating that in the absence of geldanamycin, intracellular NO production is not modified by the presence of calpain inhibitor-1 (CI-1). However, in the presence of geldanamycin, eNOS activity is also not detectable in the presence of CI-1. These results are in agreement with those shown in Fig. 2 indicating that in cells treated with geldanamycin and CI-1, eNOS was protected from degradation and was almost completely confined onto the membranes in association with caveolin-1.

Effect of Ca^{2+}-loading for a Prolonged Period of Time on the Level of eNOS and HSP90—We have previously observed that a prolonged intracellular elevation of [Ca^{2+}] induced a calpain-mediated extensive degradation of eNOS (17). To verify in the present experimental model if the protective effect of HSP90 could be overcome by prolonged calpain activation, we have exposed endothelial cells to Ca^{2+}-loading for 30 min. Under these conditions (Fig. 6, *A* and *B*), eNOS fluorescence as well as eNOS total protein levels were largely reduced both in the membrane and in the cytosolic compartment, and following the addition of geldanamycin, these digestive processes were further enhanced. As expected, after 30 min of Ca^{2+}-loading, NO synthase activity was also largely decreased (Fig. 6*C*). As expected, a higher intracellular calpain activity was detectable (for comparison see Fig. 1*E*), further indicating the involvement of the protease in the digestion of eNOS and HSP90 proteins. These data could explain the observations indicating the loss of NOS activity in dystrophic muscles (48) and the low levels of eNOS in the aorta of hypertensive rats (17).

DISCUSSION

In resting endothelial cells, the bulk of eNOS is present in an inactive form in the plasma membrane as well as in the Golgi apparatus in association with caveolin-1 (2–5, 9–11, 49, 50). Upon cell stimulation with agonists that raise the intracellular concentration of Ca^{2+}, the binding of Ca^{2+}-CAM and HSP90 to eNOS promotes dissociation from the natural inhibitor caveolin-1 and activation of the synthase in the cytosolic compartment (4, 9, 11, 19, 51). Following a decrease in $[Ca^{2+}]_i$, most of the cytosolic enzyme translocates back to the cell membrane (2, 8, 10, 12, 14, 52), indicating that the process is fully reversible.

Recent experimental evidence has provided new information on this reversible caveolin-eNOS interaction, confirming that eNOS activation occurs in response to an increase in $[Ca^{2+}]_i$ and that CAM and HSP90 are required for eNOS dissociation from the membranes and for activation of the enzyme. Moreover in reconstructed systems, it has been demonstrated that HSP90 is more efficient than CAM in displacing eNOS from caveolae (9, 11, 14).

We are presenting observations obtained by confocal microscopy and using isolated membranes confirming that translocation of eNOS from its particulate localization in the cytosol is accompanied by activation of the synthase without consumption of the enzyme. In fact, it has never been considered that even transient changes in the intracellular concentration of Ca^{2+}, besides eNOS activation, also produce translocation of active calpain at the membrane level and that native eNOS is highly sensitive to calpain digestion, which inactivates

the synthase by cleaving a peptide bond close to the CAM binding site (4, 17, 53). Thus, to protect eNOS from calpain digestion, it is reasonable to assume that under conditions of intracellular elevation of Ca^{2+}, the presence of a protective mechanism is required. The digestion by calpain might be functionally relevant, because the protease degrades, in contrast to the proteasome pathway, native enzyme forms, including active eNOS. Although digestion of NOS has been proposed as a mechanism for regulating NO production, an extensive loss of the synthase should be related to the onset of pathological states, characterized by alteration in tissue Ca^{2+} homeostasis, such as hypertension (54–59).

In the present report, we are showing that in Ca^{2+}-loaded cells, this protective mechanism involves eNOS translocation to cytosol mediated not only by Ca^{2+}-CAM but especially by functionally active HSP90. This subcellular redistribution of eNOS parallels the onset of NO production, indicating that the sequential events leading to cytosolic diffusion and subsequent activation of eNOS are dependent on its binding to HSP90. We have also demonstrated that the formation of complexes with HSP90 protects eNOS from calpain digestion; an effect promoted by the recruitment of the protease molecules in the soluble HSP90-eNOS complexes also causing the separation of these proteins from the active membrane-bound calpain. This conclusion is supported by the effect of geldanamycin, which by inhibiting HSP90 prevents the formation of the heterocomplexes, and thus calpain-mediated proteolysis of eNOS freely occurs. The protection of eNOS can be attributed to two distinct effects. The first one can be ascribed to the dissociation from the membranes that translocates the synthase away from the active protease molecules and the second to steric constraints of calpain, resulting from its binding to HSP90, which prevents degradation of both eNOS and of the chaperone protein present in the heterocomplex. All these findings are summarized in the model shown in Fig. 7, which includes the novel HSP90-based mechanism operating in the eNOS activation cycle.

Finally, our observations indicate that the function of HSP90 cannot only be related to the recovery of misfolded proteins, but also to the preservation of the native structures, increasing their resistance to proteolysis. This conclusion is supported by recent reports indicating that low molecular mass heat shock proteins exert a protective role on calpain digestion (60–62).

REFERENCES

1. Smart, E. J., Graf, G. A., McNiven, M. A., Sessa, W. C., Engelman, J. A., Scherer, P. E., Okamaoto, T., and Lisanti, M. P. (1999) *Mol. Cell. Biol.* **19,** 7289–7304
2. Goligorski, M. S., Li, H., Brodsky, S., and Chen, J. (2002) *Am. J. Physiol. Renal Physiol.* **283,** F1–F10
3. Alderton, W. K., Cooper, C., and Knowles, R. G. (2001) *Biochem. J.* **357,** 593–615
4. Kone, B. C., Kuncewicz, T., Zhang, W., and Yu, Z. (2003) *Am. J. Physiol. Renal Physiol.* **285,** F178–F190
5. Gratton, J., Bernatchez, P., and Sessa, W. C. (2004) *Circ. Res.* **94,** 1408–1417
6. Ju, H., Zou, R., Venema, V. J., and Venema, R. C. (1997) *J. Biol. Chem.* **272,** 18522–18525
7. Pott, C., Steinritz, D., Bolck, B., Mehlhorn, U., Brixius, K., Schwinger, R. H. G., and Bloch, W. (2006) *Am. J. Physiol. Cell Physiol.* **290,** 1437–1445
8. Feron, O., and Balligand, J. (2006) *Card. Res.* **69,** 788–797
9. Jiang, J., Cyr, D., Babbit, R. W., Sessa, W. C., and Patterson, C. (2003) *J. Biol. Chem.* **278,** 49332–49341
10. Ortiz, P. A., and Garvin, J. L. (2003) *Acta Physiol. Scand.* **179,** 107–114
11. Gratton, J., Fontana, J., O'Connor, D. S., Garcia-Cardena, G., McCabe, T. J., and Sessa, C. (2000) *J. Biol. Chem.* **275,** 22268–22272
12. Goetz, R. M., Thatte, H. S., Prabhakar, P., Cho, M. R., Michel, T., and Golan, D. E. (1999) *Proc. Natl. Acad. Sci.* **96,** 2788–2793
13. Michel, T. (1999) *Braz. J. Med. Biol. Res.* **32,** 1361–1366
14. Feron, O., Saldana, F., Michel, J. B., and Michel, T. (1998) *J. Biol. Chem.* **273,** 3125–3128
15. Michel, J., Feron, O., Sacks, D., and Michel, T. (1997) *J. Biol. Chem.* **272,** 15583–15586
16. Averna, M., Stifanese, R., DeTullio, R., Salamino, F., Pontremoli, S., and Melloni, E. (2008) *FEBS J.* **275,** 2501–2511
17. Averna, M., Stifanese, R., DeTullio, R., Salamino, F., Bertuccio, M., Pontremoli, S., and Melloni, E. (2008) *FEBS J.* **274,** 6116–6127
18. Stalker, T. J., Gong, Y., and Scalia, R. (2005) *Diabetes* **54,** 1132–1140
19. Stalker, T. J., Skvarka, C. B., and Scalia, R. (2003) *FASEB J.* **17,** 1511–1513
20. Osawa, Y., Lowe, E. R., Everett, A. C., Dunbar, A. Y., and Billecke, S. S. (2003) *J. Pharmacol. Exp. Ther.* **304,** 493–497
21. Su, Y., and Block, E. R. (2000) *Am. J. Physiol. Lung Cell. Moll. Physiol.* **278,** 1204–1212
22. Stifanese, R., Averna, M., Salamino, F., Cantoni, C., Mingari, M.C., Prato, C., Pontremoli, S., and Melloni, E. (2006) *Arch. Biochem. Biophys.* **456,** 48–57
23. Shao, H., Chou, C. J., Baty, N. A., Burke, S. C., Watkins, Stolz, D. B., and Wells, A. (2006) *Mol. Cell. Biol.* **14,** 5481–5496
24. Goll, D. E., Thompson, V. F., Li, H., Wei, W., and Cong, J. (2003) *Physiol. Rev.* **83,** 731–801
25. Sorimachi, H., Ishiura, S., and Suzuki, K. (1997) *Biochem. J.* **328,** 721–732
26. Xu, Y., and Mellgren, R. L. (2002) *J. Biol. Chem.* **277,** 21474–21479
27. Pontremoli, S., Melloni, E., Damiani, G., Salamino, F., Sparatore, B., Michetti, M., and Horecker, B. L. (1988) *J. Biol. Chem.* **263,** 1915–1919
28. DeTullio, R., Passalacqua, M., Averna, M., Salamino, F., Melloni, E., and Pontremoli, S. (1999) *Biochem. J.* **343,** 467–472
29. Averna, M., Stifanese, R., De Tullio, R., Passalacqua, M., Defranchi, E., Salamino, F., Melloni, E., and Pontremoli, S. (2007) *J. Biol. Chem.* **282,** 2656–2665
30. Lowry, O. H., Rosebrough, N. J., Farr, A. L., and Randall, R. J. (1951) *J. Biol. Chem.* **193,** 265–275
31. Laemmli, U. K. (1970) *Nature* **227,** 680–685
32. Palejwala, S., and Goldsmith, L. T. (1992) *Proc. Natl. Acad. Sci. U. S. A.* **89,** 4202–4206
33. Kojima, H., Nakatsubo, N., Kikuchi, K., Kawahara, S., Kirino, Y., Nagoshi, H., Hirata, Y., and Nagano, T. (1998) *Analyt. Chem.* **70,** 2446–2453
34. Nagatsubo, N., Kojima, H., Kikuchi, K., Nagoshi, H., Hirata, Y., Maeda, D., Imai, Y., Irimura, T., and Nagano, T. (1998) *FEBS Lett.* **427,** 263–266
35. Bloch, W., Mehlhorn, U., Krahwinkel, A., Reiner, M., Dittrich, M., Schmidt, A., and Addicks, K. (2001) *Nitric Oxide* **5,** 317–333
36. Michel, J. B., Feron, O., Sase, K., Prabhakar, P., and Michel, T. (1997) *J. Biol. Chem.* **272,** 25907–25912
37. Wu, W., Kao, Y., Hu, P., and Chen, J. (2007) *Exp. Eye Res.* **85,** 721–731
38. Onuoha, S. C., Mukund, S. R., Coulstock, E. T., Sengerovà, B., McLaughlin, J. S. S. H., and Jakson, S. E. (2007) *J. Mol. Biol.* **372,** 287–297
39. Bae, Y., Buresh, R. A., Williamson, T. P., Chen, T. H., and Furgeson, D. Y. (2007) *J. Control. Release* **122,** 16–23
40. Schwock, J., Pham, N., Cao, M. P., and Hedley, D. W. (2007) *Cancer. Chemother. Pharmacol.* **61,** 669–681
41. Yetik-Anacak, G., Xia, T., Dimitropoulou, C., Venema, R. C., and Catravas, J. D. (2006) *Am. J. Physiol. Heart Circ. Physiol.* **291,** H260–H268
42. Peng, X., Guo, X., Borkan, S. C., Bharti, A., Kuramochi, Y., Calderwood, S., and Sawyer, D. B. (2005) *J. Biol. Chem.* **280,** 13148–13152
43. Obermann, W. M. J., Sondermann, H., Russo, A. A., Pavletich, N. P., and Hartl, F. U. (1998) *J. Cell Biol.* **143,** 901–910
44. Grenert, J. P., Sullivan, W. P., Fadden, P., Haystead, A. J., Clark, J., Mimnaugh, E., Krutzsch, H., Ochel, H., Schulte, T. W., Sausville, E., Neckers,

L. M., and Toft, D. O. (1997) *J. Biol. Chem.* **272,** 23843–23850
45. McLaughlin, S. H., Sobott, F., Yao, Z., Zhang, W., Nielsen, P. R., Grossmann, G., Laue, E. D., Robinson, C. V., and Jackson, S. E. (2006) *J. Mol. Biol.* **356,** 746–758
46. Takahashi, S., and Mendelsohon, M. E. (2003) *J. Biol. Chem.* **278,** 9339–9344
47. Scheibel, T., Neuhofen, S., Weikl, T., Mayr, C., Reinstein, J., Vogel, P. D., and Buchner, J. (1997) *J. Biol. Chem.* **272,** 18608–18613
48. Chaubourt, E., Voisin, V., Fossier, P., Baux, G., Israel, M., and De La Porte, S. (2002) *J. Physiol. Paris* **96,** 43–52
49. Smith, A. R., Visioli, F., and Hagen, T. M. (2006) *Arch. Biochem. Biophys.* **454,** 100–105
50. Fulton, D., Fontana, J., Sowa, G., Gratton, J. P., Lin, M., Li, K. X., Michell, B., Kemp, B. E., Rodman, D., and Sessa, W. C. (2002) *J. Biol. Chem.* **277,** 4277–4284
51. Fleming, I., and Busse, R. (1999) *Cardiovasc. Res.* **43,** 532–541
52. Oess, S., Icking, A., Fulton, D., Govers, R., and Muller-Esterl, W. (2006) *Biochem. J.* **396,** 401–409
53. Govers, R., and Rabelink, T. J. (2001) *Am. J. Physiol. Renal Physiol.* **280,** 193–206
54. Mitchell, B. M., Wallerath, T., and Forstermann, U. (2007) *Methods Mol. Med.* **139,** 105–112
55. Wunderlich, C., Schmeisser, A., Heerwagen, C., Ebner, B., Schober, K., Braun-Dullaeus, R. C., Scwencke, C., Kasper, M., Morawietz, H., and Strasser, R. H. (2007) *Pulm. Pharmacol. Therap.* **21,** 507–515
56. Sud, N., Sharma, S., Wiseman, D. A., Harmon, C., Kumar, S., Venema, R. C., Fineman, J. R., and Black, S. M. (2007) *Am. J. Physiol. Lung Cell. Mol. Physiol.* **293,** L1444–L1453
57. Landmesser, U., and Drexler, H. (2007) *Curr. Opin. Cardiol.* **22,** 316–320
58. Husain, K. (2007) *Cell. Mol. Biol.* **53,** 70–77
59. Panza, J. A., Garcia, C. E., Kilcoyne, C. M., Quyyumi, A. A., and Cannon, R. O. 3rd (1995) *Circulation* **91,** 1732–1738
60. Lu, X. Y., Chen, L., Cai, X. L., and Yang, H. T. (2008) *Cardiovasc. Res.* **79,** 500–508
61. Blunt, B. C., Creek, A. T., Henderson, D. C., and Hofmann, P. A. (2007) *Am. J. Physiol. Heart Circ. Physiol.* **293,** H1518–H1525
62. Fan, G., Ren, X., Qian, J., Yuan, Q., Nicolaou, P., Wang, Y., Jones, K., Chu, G., and Kranias, E. G. (2005) *Circulation* **111,** 1792–1799